Assessing biological oxidative damage induced by graphene-based materials: An asset for grouping approaches using the FRAS assay

Salma Achawi, Bruno Feneon, Jérémie Pourchez, Valérie Forest

Assessing biological oxidative damage induced by graphene-based materials: an asset for grouping approaches using the FRAS assay.

*Salma Achawi [a,b], Bruno Feneon [a], Jérémie Pourchez [b], and Valérie Forest [b]**

[a] Manufacture Française des Pneumatiques Michelin, Place des Carmes Déchaux, 63040 Clermont-Ferrand Cedex 9, France

[b] Mines Saint-Etienne, Univ Lyon, Univ Jean Monnet, INSERM, U1059 Sainbiose, Centre CIS, F-42023 Saint-Etienne, France.

* **Corresponding author**: Valérie Forest:

Mines Saint-Etienne, 158 cours Fauriel, CS 62362, 42023 Saint-Etienne Cedex 2. France.

Email: vforest@emse.fr

Abstract

Graphene-based materials (GBMs) are extremely promising and their increasing number urges scientists to conduct more and more toxicity studies. However, case-by-case approaches are rarely the best options in the earliest phases of industrial processes. Grouping can show great assets in this context: it is defined as the process of gathering substances into a common group. Oxidative stress being a major mechanism of nanotoxicity, an important grouping criterion is the surface reactivity, for which a relevant assessment is the FRAS (ferric reducing ability of the serum) assay. However, the application of the FRAS to GBMs is questioned due to their hydrophobicity. In this study, we explored the relevance and feasibility of the FRAS for grouping, working on 22 GBMs and 2 carbon blacks. We concluded that with few adjustments, the FRAS method appeared perfectly adapted to these materials and allowed a classification as “reactive” or “non-reactive” in agreement with results of ROS production for 84% of our GBMs. While not self-sufficient for toxicity assessment, the FRAS presents interesting qualities: it is fast, cheap, and simple. Therefore, we recommend studying GBMs using the FRAS as a step of a grouping process, a complement to other assays or as an early screening tool.

Keywords: Graphene-based materials, Screening, Grouping, FRAS, Oxidative stress, Biological oxidative Damage, Surface reactivity.

1. Introduction

Graphene, a sp^2 hybridized carbon nanomaterial of one atom thickness, is considered as one of the strongest materials tested (Lee *et al.*, 2008) and has numerous other physical properties that make it among the most promising materials of this decade (Novoselov *et al.*, 2012). Its applicability is extremely wide, and its market share is planned to increase exponentially (Reiss *et al.*, 2019) positioning it as an inescapable nanomaterial for the following years. The Graphene based materials (GBMs) family is large and includes different kinds of materials such as graphene oxide (GOs), graphene nanoplatelets (GNPs) or reduced graphene oxides (rGOs) which all derived from graphite.

To ensure the integration of not only performant but also safe GBMs in the market, their toxicity needs to be thoroughly assessed. Moreover, it is now well-known that GBMs' toxicity varies depending on their physicochemical characteristics (Achawi *et al.*, 2021), which confirms the need to test each nanoform within the same family. Nanotoxicity is a challenging field: to optimize the toxicity assessment of nanomaterials and their risk management, few methods can be proposed, including grouping. Grouping is defined as the process of uniting substances into a common group if they are structurally similar with physicochemical, (eco)toxicological, and/or environmental interaction properties that are likely to be similar or to follow a regular pattern (Giusti *et al.*, 2019). This promising method could avoid laborious case-by-case approaches, but still needs more data to be completely functional (Dekkers *et al.*, 2016).

For a grouping approach, one must decide which toxicity endpoints will be considered for classification purposes. The European Centre for Ecotoxicology and Toxicology of Chemicals (ECETOC) 'Nano Task Force' proposed a decision-making framework for the grouping and testing of nanomaterials (DF4nanoGrouping) (Arts *et al.*, 2015). Its main goal is to assign nanomaterials in one of the 4 following groups depending on their expected mode of action: (1) soluble nanomaterials, (2) bio persistent high aspect ratio nanomaterials, (3) passive nanomaterials, and (4) active nanomaterials. Nanomaterials' expected mode of action is strongly dependent of their properties. Therefore, properties such as dissolution rate or *in vitro* effects can help classifying materials among the 4 classes. The classification

process also integrates bio-physical interactions such as surface reactivity. In other ECETOC approaches such as NanoApp (Janer *et al.*, 2021) which aims to create sets of similar nanoforms, surface reactivity (which can be measured with FRAS, EPR or DCF assay) is also one of the criteria that can be used to classify nanoforms as similar.

Returning to the GBMs, the grouping method could be a great asset as it would represent an early toxicity assessment, allowing industries and scientists to focus on materials that appear to show a minor toxicity impact. GBMs' most well-known mode of action is oxidative stress (Mittal *et al.*, 2016) (Pelin *et al.*, 2018) (Ou *et al.*, 2016) which can be measured by various analytical methods: *in vitro* cellular testing can for example measure the production of reactive oxygen species or the depletion of antioxidants induced by the nanomaterial while cell free assays can be useful for measuring nanomaterial's intrinsic reactive potential or the biological oxidative damage produced on human matrix. Among these methods, the FRAS (Ferric reducing ability of the serum) assay was pointed as particularly interesting in view of its sensitivity (Hellack *et al.*, 2017).

The FRAS assay measures biological oxidative damage produced on a human matrix through the measurement of the surface reactivity of a nanomaterial in cell free conditions. Available surface of nanomaterials being one of their most important aspect impacting toxicity (Karakoti *et al.*, 2006), surface reactivity has a major role in all types of interaction with the environment, strongly driving health hazard (Magro *et al.*, 2018) (Warheit, Reed and Sayes, 2009). A method published in 1996 described the ferric reducing ability of plasma (FRAP) (Benzie and Strain, 1996) and aimed to measure the antioxidant power of a chosen biological matrix: plasma. Serum was then presented as an interesting alternative to plasma as it does not include coagulation factors which can cause interferences with the assay (Rogers *et al.*, 2008). The FRAP assay finally became the FRAS assay. Other approaches exist, such as the FRAN (ferric reducing ability of nanoparticles) where redox reactions are observed directly on nanoparticles' surface (Bi and Westerhoff, 2019).

FRAS protocol shows interesting assets as it is simple, reproducible and already widely used to measure the antioxidant capacity of a biological matrix in the framework of clinical studies (Gawron-Skarbek *et*

al., 2019) or *in vivo* measurements (Cecchini and Fazio, 2020). However, in the framework of DF4 nanogrouping, surface reactivity of GBMs could not be assessed using FRAS, which was considered unsuitable for such insoluble materials (Arts *et al.*, 2016). GBMs were indeed not expected to disperse properly enough to be able to observe any change in the exposed serum properties.

Gandon *et al.* recently published a protocol of the FRAS measurement, adapted for grouping or read across methods, and optimized for nanomaterials (Gandon *et al.*, 2017). We worked on this protocol, and slightly modified it. Using a wide range of GBMs, we demonstrated the feasibility of FRAS assay for GBMs Moreover, we aimed to make this protocol even easier to work with by thoroughly describing the protocol step by step. Lastly, we intended to propose a quicker version of this protocol, enabling us to work on 3 nanomaterials a day.

In this paper, we demonstrate that an adapted FRAS protocol can be a fast, straightforward, and efficient way to measure GBMs' surface reactivity. We also discuss the relevance of FRAS assay as a grouping endpoint by comparing its results to the ROS production measured in a macrophage cell line through the DCF-DA assay.

2. Material and Methods

2.1. Nanomaterials

To evaluate the feasibility of FRAS assay on GBMs we used a wide range of GBMs, espcially graphene nanoplatelets (GNPs) and reduced graphene oxide (rGO). Their specific surface area (SSA) was determined with BET technique (adsorption of nitrogen, with degassing system Micromeritics). Their surface oxidation was determined with XPS (X-ray Photo spectroscopy, Quantera Scanning XPS microprobe, Physical Electronics). Lateral size was determined with electronic microscopy (Field Emission Scanning Electron Microscope, from JEOL). ID/IG ratio was calculated with RAMAN spectroscopy (XploRA, Horiba Scientific). For comparison, we also tested two samples of carbon black (CB) and one sample of amorphous silica and Mn_2O_3 as positive control. All these samples are listed in Table 1. In supplementary data 1, ICP and XPS analyses and the RAMAN spectra are reported.

Table 1 - Samples tested in our study and their physicochemical characterization.

	Surface Oxidation (% O)	Mean Lateral Size (µm)	Surface defects (ID/IG)	Specific Surface Area (m^2/g)
GNP1	3.2	1.25	0.369	283
GNP2	6.3	0.66	0.470	439
GNP3	7.6	0.53	0.724	692
GNP4	4.3	3.56	0.340	38
GNP5	3.3	5.58	0.062	41
GNP6	2.6	7.91	0.146	48
GNP7	4.2	10.86	0.101	89
GNP8	5.9	17.34	0.634	168
GNP9	5.7	38.57	0.068	119
GNP10	2.1	33.54	0.132	34
GNP11	2.5	30.70	0.225	31
GNP12	6.1	1.63	0.348	396
GNP13	4.4	3.16	0.645	125
GNP14	4.5	1.51	0.346	335
GNP15	3.5	2.02	0.321	255
rGO3	11.9	8.26	1.038	545
rGO4	7.2	31.56	0.937	880
rGO5	2.7	6.99	1.066	830
rGO6	15.9	32.01	0.905	270
rGO7	6.7	15.1	0.957	810
rGO8	17.2	1.04	0.908	440
rGO9	2.6	1.11	1.066	870
CB1	2.6	0.36	NA	112
CB2	2.3	0.9	NA	85
Amorphous Silica	70.0	0.09	NA	160
Mn_2O_3 (grade 1)	NA	NA	NA	1.7
Mn_2O_3 (grade 2)	NA	NA	NA	18.7

2.2. Development of a FRAS assay protocol adapted to GBMs

The principle of this method is to measure the antioxidant ability of a matrix exposed to a chemical through the observation of its ferric reducing capacity. The ferric reducing capacity can be considered as an analog of the antioxidant power (Hsieh *et al.*, 2013) (Piątek-Guziewicz *et al.*, 2017). Indeed, the chemical reaction of taking an electron from an atom is oxidation, whereas the opposite chemical reaction of giving an electron to an atom is the reduction. Hence, the FRAS assay principle is to measure

the capacity of a serum sample which has been exposed to nanomaterials (or any other chemicals) to reduce ferric ions to ferrous ions. Figure 1 briefly presents the concept of the FRAS assay.

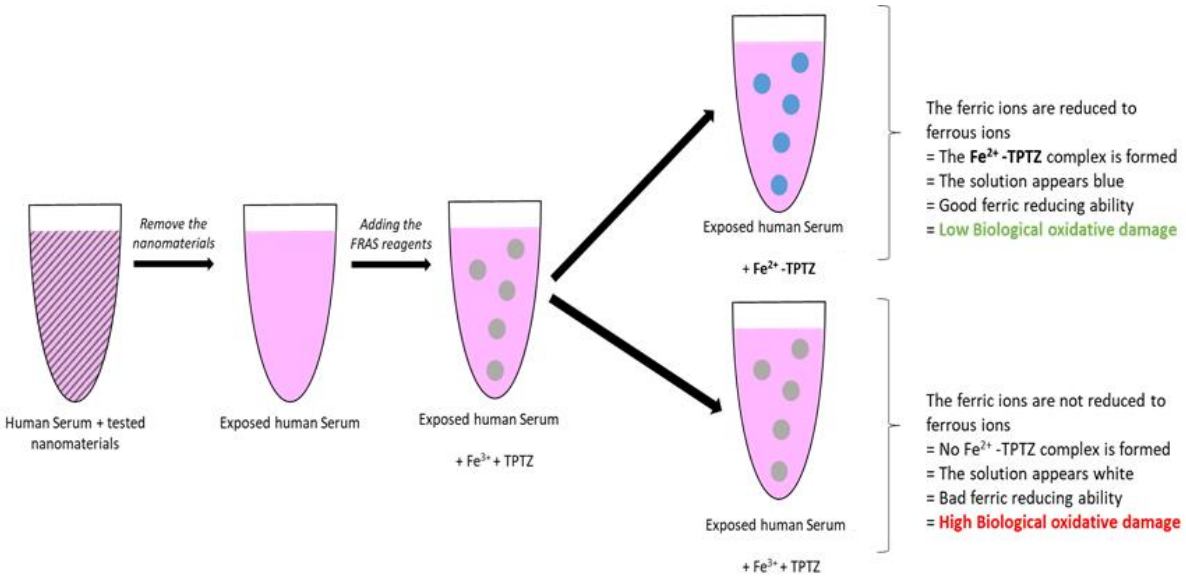

Figure 1: Presentation of the FRAS assay.

Our protocol is driven by the work of Gandon *et al.* published in 2017. We present the full protocol in supplementary data 2 and list necessary equipment and chemicals in supplementary data 3. Briefly, we prepared solutions of human blood serum and nanomaterials at concentration of 5, 10 and 20 g/L. We incubated the HBS-NM solutions during 3 hours at 37°C (ThermoMixer, Fisher). We then separated the NM from the exposed human blood serum though a centrifugation (Heraeus Megafuge Centrifuge, Thermo). Lastly, we collected the HBS supernatant and added it to FRAS reagent, allowing FRAS reaction. After a 60-minute reaction time, we measured the absorbance (Spectrophotometer MULTISKAN, Thermo) of each sample (see supplementary data 4 for labelling the vials for this assay). We modified few steps from the protocol from Gandon *et al*. to optimize this assay to our needs and the use on GBMs. These modifications are described in supplementary data 2.

To analyze the data, a calibration curve was established using Trolox, an equivalent of vitamin E (see calibration step in supplementary data 2, and analysis section 2.4.1).

2.3. Specificities of low density GBMs

We worked on a wide range of GBMs to make sure that this method was feasible for all of them. We encountered some difficulties with very low density GBMs. Some rGOs have a very low density and preparing a high concentration with these nanomaterials can be challenging especially when the powders occupied a larger volume than the HBS. In these conditions, we did not prepare 20 g/L concentrations for rGO4, rGO5, rGO6, rGO7, rGO8 and rGO9. The sonication, incubation and centrifugation were strictly the same as for the other tested items. Separating the HBS from the nanomaterials was the most challenging part: our centrifuge could not reach the 11,900 rpm initially required by the protocol written by Gandon *et al.*, and the low density prevented us from removing the nanomaterials before addition of the FRAS reagent. We then chose to separate these particular GBMs with an additional step: after the centrifugation, we collected the supernatant and then filtered it with a syringe filter of 0.2 µm to eliminate the remaining nanomaterials (see supplementary data 5).

2.4. Analysis

2.4.1. TROLOX calibration

This step is essential to convert our results into Trolox equivalent unit (TEU). Trolox ($C_{14}H_{18}O_4$) is a water-soluble analog of vitamin E and a well-known antioxidant(Arts *et al.*, 2004). To test the ferric reducing ability of our serum exposed to this antioxidant, we replaced the HBS previously exposed to nanomaterials by a series of concentrations of Trolox in water of 0.1, 0.05, 0.01, 0.005 and 0.001 g/L. We obtained a FRAS absorption signal that can be linearly fitted with the equation:

$$\mathbf{Abs_{Trolox} = k\varepsilon * l * d * C_{Trolox} + b \ (R^2 = 0.9998).}$$

Where:

- Abs = Absorption [Arbitrary units]
- l = light path of cuvette [cm]: 0.3 cm in our case.
- kε = extinction coefficient of the complex Fe^{2+}/ TPTZ induced by 1 Mol antioxidant [Trolox equivalent unit, TEU]

- d = dilution factor 0.048 (0.1 ml HBS in 2 ml FRAS reagent)
- C_{Trolox} = concentration [mM]

In our case, kE*l*d was **1.9625** and b, our offset, was **0.0488**. In comparison, Gandon *et al.* obtained kE*l*d = **2.654** and an offset of **0.075**. Please note that the light path of their cuvette was 10 mm whereas our cuvette measured 3 mm. These data are consistent with our values.

Concretely, we will use these data to convert absorbance units to Trolox equivalent units, enabling us to compare the results between each study. It also enables us to calibrate our test according to the HBS used and the different batches provided. Therefore, if you are using more than one bottle of HBS, consider performing this calibration step for each bottle.

2.4.2. Conversion in Biological oxidative damage (BOD) surface-based BOD and mass-based BOD

The main results that we can obtain from the FRAS assay are:

- Biological oxidative damage (BOD) [in mM TEU]: obtained directly with the absorbance and converted in TEU as shown in part 2.4.1.
- Mass-based biological oxidative damage (m-BOD) [in nMTEU /mg]: obtained by dividing BOD by its concentration [in g/L].
- Surface-based biological oxidative damage (s-BOD) [in nMTEU /m²]: obtained by dividing the BOD by the dose of nanomaterial (a combination of its concentration [in g/L] and specific surface area [in m²/g]).

The equations and explanations for obtaining these values are described in Gandon *et al*. Moreover, we present a step-by-step analysis of an example in supplementary data 6.

2.4.3. Positive control

In the frame of the DF4 nano grouping, nanomaterials are classified depending on Mn_2O_3 surface reactivity: this material is indeed the preferred positive control as it is reactive for FRAS assay, band

gap analysis (Zhang *et al.*, 2012) and cytochrome c assay (Delaval *et al.*, 2016). For the grouping method published by Arts et al., as well as the work of Gandon et al., a specific grade of Mn_2O_3 (with a specific surface area of 19.9 m^2/g) was used. Unfortunately, this reference is not available anymore. For the sake of a good standardization, we aimed to test the BOD caused by Mn_2O_3 within our own experiments. We ordered two different grades of Mn_2O_3, differing by their dimension and specific surface area:

- Mn_2O_3 Grade 1: SSA = 1.7 m^2/g, particle size 325 mesh (equals to approximately 44 µm).
- Mn_2O_3 Grade 2: SSA = 18.7 m^2/g, particle size 60 nm.

With these two samples, we aimed to show how using various grades of the same chemical could impact the results and to test a grade of Mn_2O_3 that showed close SSA to the one used in the existing literature.

2.5. DCFDA Assay

We wanted to study the potential correlation between the biological oxidative damage induced by NM and their ROS cellular production. To this end, we performed a DCFDA assay to measure the ROS production caused by the exposure of cells to the same GBMs.

RAW 264.7 murine macrophage cell line was provided by ATCC Cell Biology Collection (Promochem LGC). It derived from mice peritoneal macrophages transformed by the Albeson Murine Leukemia Virus. Cells were grown in 10% fetal calf serum Dulbecco's Modified Eagle Medium (DMEM, Invitrogen) supplemented with 1% penicillin-streptomycin (Sigma-Aldrich) and maintained at 37°C under a 5% carbon dioxide humidified atmosphere. Cells were exposed to increasing concentrations of GBMs (from 15 to 120 µg/mL) for 90 minutes. We then measured the ROS production through the OxiSelect™ Intracellular ROS Assay Kit (STA-342).

3. Results

3.1. Biological oxidative damage induced by GBMs

Gandon *et al.* recommends plotting each series of replicates for each nanomaterial with log (Dose) on x-axis and log (BOD) on y-axis and to fit with a linear regression curve. However, for reactive materials, a linear curve might not be appropriated and could be replaced with a sigmoid. Indeed, we did not have very good fits for reactive GBMs. We hence decided to calculate a mean BOD (Figure 2A), and sBOD (Figure 2B). Note that for low-density GBMs, we could not prepare a 20 g/L solution (see section 2.3).

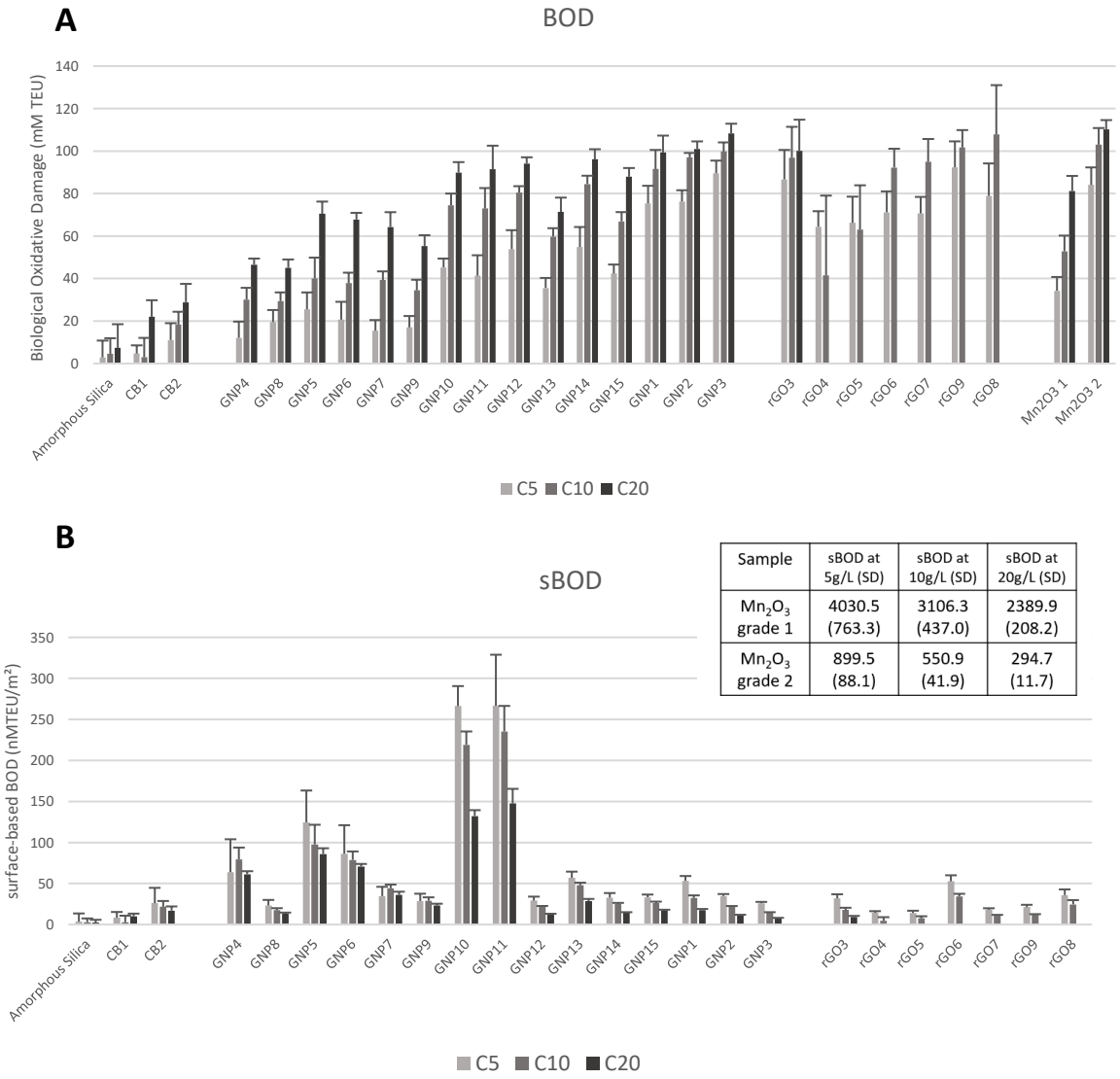

Sample	sBOD at 5g/L (SD)	sBOD at 10g/L (SD)	sBOD at 20g/L (SD)
Mn_2O_3 grade 1	4030.5 (763.3)	3106.3 (437.0)	2389.9 (208.2)
Mn_2O_3 grade 2	899.5 (88.1)	550.9 (41.9)	294.7 (11.7)

Figure 2: A) Biological oxidative damage (BOD) and B) Surface-based Biological Oxidative Damage (sBOD) (note that the results of Mn_2O_3 are presented in a table since the scale was extremely different).

The biological oxidative damage values induced by GBMs, CB and the amorphous silica are variable and dose dependent. Overall, we can conclude that FRAS assay efficiently measures the BOD induced by various types of GBMs and allows a certain classification of GBMs between each other. However, for some samples (GNP3, rGO3 or Mn_2O_3 grade 2), a maximum BOD of approximately 100 mMTEU is reached from the lowest dose (5 g/L). As the dose increases, no dose response appears which indicates a probable saturation effect around 100 mMTEU.

Concerning mBOD, as almost every nanomaterial shows a dose dependent BOD, the highest mBOD can often be measured at 5 g/L and can reach 18.5 nMTEU/mg. The values are in the same range than the one previously published (see section 4.1 of discussion).

The sBOD allows considering the surface reactivity for each square meter of material. As shown in section 2.4.2 of Material and methods, it includes the specific surface area and the concentration of the GBMs. We mostly obtain a maximum sBOD at the dose of 5 g/L. The sBOD are extremely variable, between 0 and 350 nMTEU/m^2. Grades 1 and 2 of Mn_2O_3, have low SSAs (1.7m^2/g and 20m^2/g) while having strong BODs (up to 81 and 110 mTEU respectively), which automatically leads to an extremely high sBOD (from 2090 to 4010 nMTEU/m^2). Hence, the two chosen grades of Mn_2O_3 show an extremely high sBOD compared to GBMs, CBs and the amorphous silica.

Overall, even with reactive materials such as GBMs, this assay appears to successfully classify GBMs as reactive or not concerning biological oxidative damage.

3.2. Biological oxidative damage and ROS production induced by GBMs

For a simple presentation of the results, we chose to present only one exposure concentration for each assay: 5 g/L for FRAS assay and 120 µg/mL for DCFDA assay. Also, the FRAS results are indicated in BOD whereas the DCFDA are presented in fold to negative control. The results are presented in Figure 3.

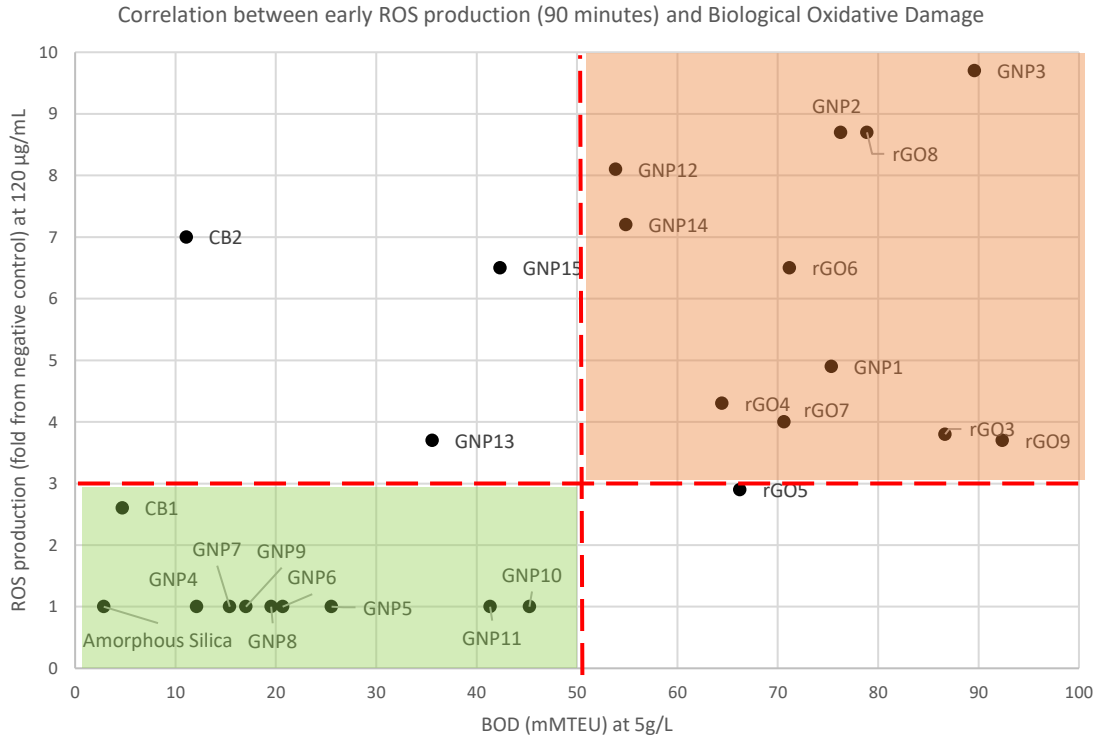

Figure 3: Correlation between early reactive oxygen species (ROS) cellular production and biological oxidative damage (BOD). Early ROS cellular production is considered as high when it hits 3 times the negative control and BOD is considered high when it hits 50 mMTEU. Nanomaterials that have a high ROS production and a high BOD are considered reactive, whereas the ones with low to moderate ROS and BOD are considered non-reactive.

Firstly, we can note a link between the ROS production and the BOD caused by the GBMs. Two main groups of GBMs can also be described. The first one, in green, gathers 10materials exhibiting a low ROS production at high concentration (90 minutes of exposure to 120 µg/mL) and a low to moderate BOD. The second group, in orange, gathers 11 nanomaterials that show a high BOD combined with an increased ROS production. For information, the tendency is the same for a ROS production measured after a 24-hour exposure time. 4 materials cannot be classified in one of these groups, one of them being a carbon black.

In conclusion, we can consider that the combination of DCFDA and FRAS appears as an interesting methodology for classifying materials as “reactive” or “non-reactive” for a grouping approach.

4. Discussion

4.1. Values in the literature for FRAS assays

In the literature, there are only few studies of the FRAS assessment for GBMs or CBs. The papers presenting such results to our knowledge are presented in supplementary data 7. Please note that for an easier reading, all results were converted in the same unit: nM TEU.

Some CBs had their BOD, sBOD and mBOD measured. In our tested samples, the two tested CBs have approximately the same SSA than CB N110. Both our CBs showed a very moderate FRAS effect. We found that for CB1, BOD equals 2.99 mMTEU, sBOD equals 2.7 nMTEU/m² and mBOD equals 1.11 nMTEU/mg. In the work published by Hsieh et al (2012), the CB N110 had a mean BOD of 0.937 mMTEU, a sBOD of 80 nMTEU/m² and mBOD of 9 nMTEU/mg. These results differ but remain in the same range for BOD.

Concerning GBMs, only Hsieh et al (2013) investigated these materials. A GBM with a SSA around 100 m²/g was tested, which could be transposed to GNP9 or GNP15. We do not have a lot of information on the result of physicochemical characterization, so we are relying our comparison on SSA. We found that GNP15 has a sBOD of 48.2 nMTEU/m² and a mBOD of 6 nMTEU/mg and GNP9 has a sBOD of 29.2 nMTEU/m² and a mBOD of 3.5 nMTEU/mg. In the work of Hsieh *et al* (2012), their 2 GBMs had a sBOD of 92 and 103 nMTEU/m² and a mBOD of 9 and 10 nMTEU/mg. These results are quite consistent, GNP15 showing closer results with the two tested GBMs in Hsieh et al (2012).

Overall, comparable nanomaterials present the same range of results. The variations can be due to multiple factors: the protocol used that differed, the grade of chemicals used and the grade and source of human blood serum (see supplementary data 8 for blank antioxidant capacity of the serum measurement).

4.2. Correlation between biological oxidative damage and ROS production

FRAS and DCF-DA assay measure different biological endpoints. FRAS acellular assay measures the reducing activity of a serum previously exposed to chemicals which is a proxy of its antioxidant capacity or the biological oxidative damage (BOD) induced by a chemical. DCF-DA is a cellular assay which measures the ROS production of cells previously exposed to chemicals. We performed this assay on murine macrophages (RAW264.7) since these cells are ubiquitous and specialized in foreign substances' elimination.

We observed a potential correlation of the results of these two assays. Two major groups can be distinguished: a group that shows a low pro-oxidant capacity and moderate BOD and a group that shows a high pro-oxidant capacity and high BOD. A vast majority of our samples can be classified in one of these groups. Even if these two assays do not measure the same biological endpoint, it seems that the results of DCF-DA and FRAS assay are quite well-correlated.

Our results are in agreement with a study (Pal *et al.*, 2014) where a correlation was found between an acellular DCF-DA results and a FRAS assay for diverse nanomaterials. This tendency was strengthened with the cellular oxidative stress measurement performed on seven NMs (GSH: GSSG assay performed on THP-1) which appeared to be correlated to the FRAS results.

Recently, different methods for assessment of surface reactivity were tested on a total of 35 nanomaterials (Bahl *et al.*, 2020). A combination of an acellular assay such as FRAS and a cellular assay such as protein carbonylation was found to be an excellent approach for categorization.

These conclusions place FRAS assay as a useful step for surface reactivity measurement which itself, through grouping, is a critical step for nanomaterials hazard assessment.

4.3. Classification with Mn_2O_3 in the context of DF4 nanogrouping

The positive control of this assay (Mn_2O_3) is particularly important since it allows the classification of the tested samples as "reactive" or "non-reactive" by delimiting a threshold based on its sBOD. In the workflow of DF4 nanogrouping, the measured sBOD of Mn_2O_3 was 192.2 nMTEU/m². Above the limit

of 10% of this sBOD, the nanomaterials are classified as reactive, which will classify them as group 4, “active nanomaterials”.

The classification as reactive or not is relative to the reactivity of a positive control. We can assume that the protocol used, the reagents used, and the grade of the biological matrix used can interfere in the measured BOD. Therefore, we would advise every team working on a FRAS assay to measure the BOD caused by Mn_2O_3 with the same protocol and the same chemicals used as for the measurement of the rest of the nanomaterials.

Moreover, note the importance of carefully choosing the right grade of Mn_2O_3. Consider choosing the nanoscale as the most relevant positive control for nanoparticles: its specific surface area must be close to the samples tested. In our case, we tested a microscale Mn_2O_3 (grade 1) and a nanoscale Mn_2O_3 (grade 2). These two samples caused variable but still comparable BOD (up to 110 mMTEU for nanoscale Mn_2O_3 and 88 mMTEU for micro-scale Mn_2O_3). However, their variation of SSA (1.7 m^2/g VS 20 m^2/g) automatically leads to an increased sBOD: for each square meter, the microscale grade of Mn_2O_3 seems to cause more BOD.

Overall, these two grades of Mn_2O_3 lead to a much higher sBOD than the one considered for classification in the context of DF4 nanogrouping. The closest Mn_2O_3 to the one used in the existing literature we could find is the grade 2 (SSA=18.7 m^2/g) and led to a BOD of 103 mMTEU and a sBOD of 550.9 nMTEU/m^2 which is higher than 192.2 nMTEU/m^2.

This major gap highlights the importance of considering the grade and source of chemicals used in assay, especially if a chemical is used as a control and/or for classification purposes.

In a grouping methodology, the FRAS assay needs to be standardized with a threshold splitting the materials as reactive or not. If we consider the threshold given by Arts et al., our CBs, amorphous silica and 7 of our GBMs (mostly rGOs) are classified as non-reactive while 15 GBMs can be classified as reactive.

Briefly, the decision-making framework of nanogrouping stands on three tiers, presented in Figure 4.

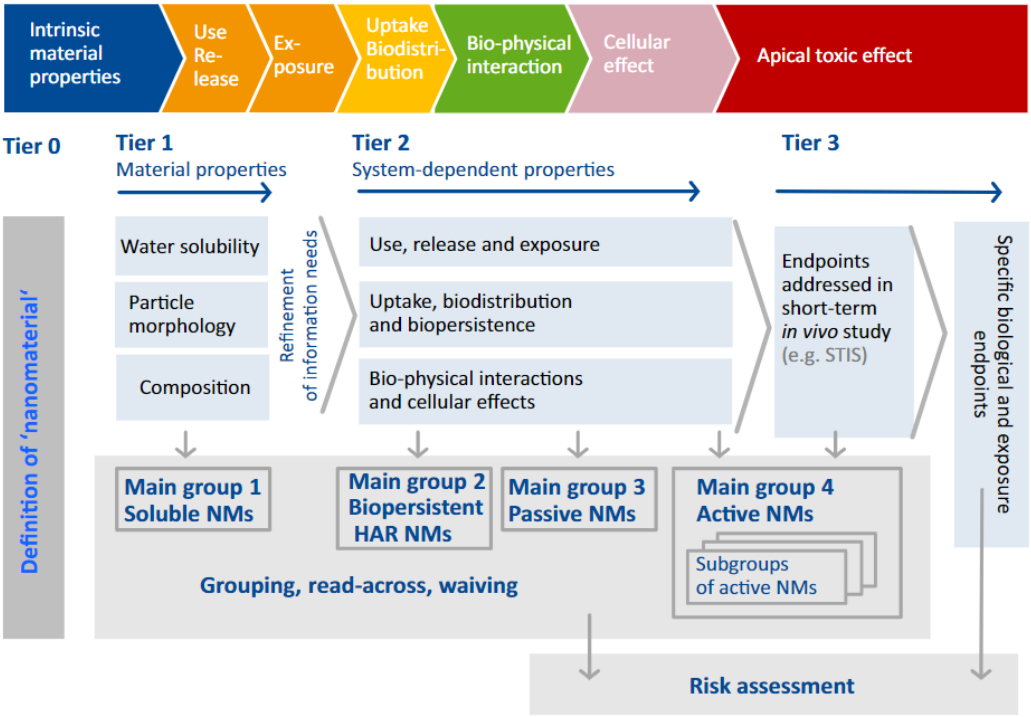

Figure 4: The decision-making framework for the grouping and testing of nanomaterials (DF4nanoGrouping). Reproduced with permission.

The major grouping criteria are solubility, aspect ratio, surface reactivity (measured through FRAS assay) and cellular effect. The FRAS assay is hence only one step of a global grouping process.

For the first tiers, GBMs showed no solubility, excluding them from group 1 "soluble materials", GBMs do not present the properties of a HARP (high aspect ratio particle) and are not fibers, making the classification in group 2 "Biopersistent, HAR nanomaterials" irrelevant. In tier 2, surface reactivity could not be assessed due to the lack of knowledge about FRAS assay for graphene-based materials. In the case study presented by Arts et al., this data gap led to exclude GBMs from group 3 "Passive nanomaterials" and to classify them as group 4 "Active nanomaterials" by conservative default. The same graphite nanoplatelets as the one assessed in this case study were tested in another study and was classified as "passive" for cellular effects (Wiemann *et al.*, 2016), yet still remained in group "Active nanomaterial", because of a lack of knowledge considering its FRAS effect.

With our results, 7 GBMs showed a surface reactivity lower than the DF4 quantitative threshold (sBOD < 19.2 nTEU/m²), possibly allowing them to be classified in group 3 “passive nanomaterials”.

With our measurements, we now know that some GBMs can be classified as non-reactive (concerning their surface reactivity). Therefore, performing the FRAS assay for GBMs can avoid data gaps which often lead to over classification.

4.4. Feasibility and relevance of FRAS assay for graphene-based materials

The assessment of biological oxidative damage (BOD) is an essential grouping criterion in the frame of DF4 nanogrouping, participating to the classification as “active” or “passive” nanomaterial, which will dramatically change its final risk assessment.

In addition, the FRAS assay is interesting as it can act as a screening test before heading to a complete toxicity assessment and does not require working in a cell culture lab. In a context of very high interest and demand for nanomaterials, including graphene-based materials (GBMs), there are often a great number of potential candidates to integrate into industrial process or to study further. A case-by-case approach for a complete toxicity assessment, including *in vitro* and *in vivo* testing, is often not relevant for very early stages of research and development. In this context, straightforward, cheap, and accessible methods such as FRAS assay can be a first step for a toxicity screening.

The protocol presented in supplementary data 2 enables to test 3 nanomaterials each day. We then needed a total of 3 to 4 weeks to perform the testing of 27 different samples and the calibration of the assay with the Trolox.

An important point we observed in our study is the saturation at approximately 100 mMTEU. In this regard, when testing very reactive samples such as GBMs, it might not be relevant to test concentrations higher than 10 g/L. If a very quick screening of a great number of samples is needed, one could consider studying only a 10 g/L concentration (since it is the most commonly used dose in the literature and could allow easier inter-lab comparison) and having only one vial of blank each day. This way, it could be possible to test up to 11 nanomaterials in only one day. Another interesting

approach would be to test one single surface dose of 1 m^2/L and is described in a paper presenting nanoGRAVUR framework (Wohlleben *et al.*, 2019). Lastly, for assessing the dose response of reactive materials, the FRAS assay can be performed using the same concentrations used for Trolox calibration (from 0.001 g/L to 0.1 g/L, see section 2.4.1). This method allows a linear fit of the FRAS signal and avoids any saturation effect (Peijnenburg *et al.*, 2020).

In this paper, we focused on GBMs. However, we also tested 2 carbon blacks with good results in terms of feasibility. This is an interesting information since these nanomaterials are often used at an important tonnage, carbon black being the most produced carbon-based nanostructure (Khodabakhshi, *et al.*, 2020). Hence, these results can also indicate that the used FRAS protocol is adapted not only to GBMs, but also to carbon blacks.

Considering their mode of action involving oxidative stress and their very high specific surface area, assessing surface reactivity of GBMs is relevant. With our results, we showed that this assay was selective on a wide variety of samples. We obtained a FRAS response for almost all our tested GBMs, which can make us consider that their poor dispersibility was not an obstacle for this assay. Moreover, we highlighted a potential correlation between the results of early ROS production and FRAS assays: the GBMs that show an increased production of ROS are often the same ones that cause a high biological oxidative damage. These results can help us to consider FRAS as an interesting assay for nanoparticles with mode of action involving oxidative stress.

However, we can mention few limitations for our study. We aimed to study as many GBMs as possible, with different physico-chemical characteristics. However, we did not include GOs (graphene oxides). Since the FRAS assay was considered inappropriate for materials that interfered with the optical read-out due to their black color and their lack of dispersibility, we focused on GBMs with a very low dispersibility, being mostly GNPs and rGOs. Knowing that GOs, due to their high oxidation state and their quite small lateral size (compared to our samples which can measure up to 30 µm), have been shown to have a better dispersibility than rGO (Konios *et al.*, 2014) (Johnson *et al.*, 2015), we can assume that if FRAS is feasible on very insoluble materials such as GNPs, it is probably feasible on quite

soluble materials such as GOs. It might be yet necessary to test this assay on a few samples of GOs in the future to confirm this hypothesis.

5. Conclusion

As graphene based materials (GBMs) market share and global interest for application is growing, it became urgent to explore its potential toxicity. However, a case-by-case approach is often irrelevant in the earliest phases of the industrial process whereas quick and simple assays for early toxicity screening can be appropriate. These assays can also be integrated into a global process, such as grouping.

FRAS (ferric reducing ability of the serum) assay shows interesting assets: it is a simple assay, accessible and fast. Moreover, its reproducibility was previously studied, and its protocol have been optimized for nanomaterials. Yet, its feasibility on GBMs was questioned, due to the hydrophobicity of these samples.

We tested 25 samples, including 22 GBMs, 2 carbon blacks and 1 amorphous silica and measured their FRAS effect. We found various biological oxidative damage (BOD) caused by these samples. Overall, it appeared that FRAS was not only feasible on GBMs but represented a critical step for classification in the context of DF4 nanogrouping. FRAS assay cannot be considered as a single assay for measuring GBMs toxicity. However, it can be considered as a screening tool, or complement other toxicity assays.

Funding

This work was supported by Michelin.

List of abbreviations

- FRAS : Ferric reducing ability of the serum
- GBMs : Graphene-based materials
- DCFDA : Dichlorodihydrofluorescein Diacetate

- EPR : Electron paramagnetic resonance
- ECHA : European chemicals agency
- FRAP : Ferric reducing ability of the plasma
- NM : Nanomaterials
- HBS : Human blood serum
- GNPs : Graphene nanoplatelets
- rGOs : Reduced graphene oxide
- GOs : Graphene oxide
- TEU : Trolox equivalent unit
- BOD : biological oxidative damage
- sBOD : Surface-based biological oxidative damage
- mBOD : Mass-based biological oxidative damage
- SSA : Specific surface area
- HARP : High aspect ratio particles
- ECETOC : European Centre for Ecotoxicology and Toxicology of Chemicals
- ROS : Reactive oxygen species

References

Achawi, S. *et al.* (2021) 'Graphene-Based Materials In Vitro Toxicity and Their Structure–Activity Relationships: A Systematic Literature Review', *Chemical Research in Toxicology*. doi: 10.1021/ACS.CHEMRESTOX.1C00243.

Arts, J. H. E. *et al.* (2015) 'A decision-making framework for the grouping and testing of nanomaterials (DF4nanoGrouping)', *Regulatory Toxicology and Pharmacology*, 71(2), pp. S1–S27. doi: 10.1016/j.yrtph.2015.03.007.

Arts, J. H. E. *et al.* (2016) 'Case studies putting the decision-making framework for the grouping and testing of nanomaterials (DF4nanoGrouping) into practice', *Regulatory Toxicology and Pharmacology*, 76, pp. 234–261. doi: 10.1016/j.yrtph.2015.11.020.

Arts, M. J. T. J. *et al.* (2004) 'Antioxidant capacity of reaction products limits the applicability of the Trolox Equivalent Antioxidant Capacity (TEAC) assay', *Food and Chemical Toxicology*, 42(1), pp. 45–49. doi: 10.1016/j.fct.2003.08.004.

Bahl, A. *et al.* (2020) 'Nanomaterial categorization by surface reactivity: A case study comparing 35 materials with four different test methods', *NanoImpact*, 19, p. 100234. doi: 10.1016/j.impact.2020.100234.

Benzie, I. F. F. and Strain, J. J. (1996) 'The ferric reducing ability of plasma (FRAP) as a measure of "antioxidant power": The FRAP assay', *Analytical Biochemistry*, 239(1), pp. 70–76. doi: 10.1006/abio.1996.0292.

Bi, X. and Westerhoff, P. (2019) 'Ferric reducing reactivity assay with theoretical kinetic modeling uncovers electron transfer schemes of metallic-nanoparticle-mediated redox in water solutions', *Environmental Science: Nano*, 6(6), pp. 1791–1798. doi: 10.1039/C9EN00258H.

Cecchini, S. and Fazio, F. (2020) 'Assessment of total antioxidant capacity in serum of heathy and stressed hens', *Animals*, 10(11), pp. 1–8. doi: 10.3390/ani10112019.

Dekkers, S. *et al.* (2016) 'Towards a nanospecific approach for risk assessment', *Regulatory Toxicology and Pharmacology*, 80, pp. 46–59. doi: 10.1016/j.yrtph.2016.05.037.

Delaval, M. *et al.* (2016) 'Assessment of the oxidative potential of nanoparticles by the cytochrome c assay: assay improvement and development of a high-throughput method to predict the toxicity of nanoparticles', *Archives of Toxicology 2016 91:1*, 91(1), pp. 163–177. doi: 10.1007/S00204-016-1701-3.

Gandon, A. *et al.* (2017) 'Surface reactivity measurements as required for grouping and read-across: An advanced FRAS protocol', in *Journal of Physics: Conference Series*. Institute of Physics Publishing, p. 12033. doi: 10.1088/1742-6596/838/1/012033.

Gawron-Skarbek, A. *et al.* (2019) 'The influence of an eight-week cycloergometer-based cardiac rehabilitation on serum antioxidant status in men with coronary heart disease: A prospective study', *Medicina (Lithuania)*, 55(4). doi: 10.3390/medicina55040111.

Giusti, A. *et al.* (2019) 'Nanomaterial grouping: Existing approaches and future recommendations', *NanoImpact*. Elsevier B.V., p. 100182. doi: 10.1016/j.impact.2019.100182.

Hellack, B. *et al.* (2017) 'Analytical methods to assess the oxidative potential of nanoparticles: A

review', *Environmental Science: Nano*. Royal Society of Chemistry, pp. 1920–1934. doi: 10.1039/c7en00346c.

Hsieh, S. F. *et al.* (2013) 'Mapping the biological oxidative damage of engineered nanomaterials', *Small*, 9(9–10), pp. 1853–1865. doi: 10.1002/smll.201201995.

Janer, G., Landsiedel, R. and Wohlleben, W. (2021) 'Rationale and decision rules behind the ECETOC NanoApp to support registration of sets of similar nanoforms within REACH', *Nanotoxicology*, 15(2), pp. 145–166. doi: 10.1080/17435390.2020.1842933.

Johnson, D. W., Dobson, B. P. and Coleman, K. S. (2015) 'A manufacturing perspective on graphene dispersions', *Current Opinion in Colloid and Interface Science*. Elsevier Ltd, pp. 367–382. doi: 10.1016/j.cocis.2015.11.004.

Karakoti, A. S., Hench, L. L. and Seal, S. (2006) 'The potential toxicity of nanomaterials - The role of surfaces', *JOM*. Springer, pp. 77–82. doi: 10.1007/s11837-006-0147-0.

Khodabakhshi, S., Fulvio, P. F. and Andreoli, E. (2020) 'Carbon black reborn: Structure and chemistry for renewable energy harnessing', *Carbon*, 162, pp. 604–649. doi: 10.1016/J.CARBON.2020.02.058.

Konios, D. *et al.* (2014) 'Dispersion behaviour of graphene oxide and reduced graphene oxide'. doi: 10.1016/j.jcis.2014.05.033.

Lee, C. *et al.* (2008) 'Measurement of the Elastic Properties and Intrinsic Strength of Monolayer Graphene', *Science*, 321(5887), pp. 385–388. doi: 10.1126/science.1157996.

Magro, M. *et al.* (2018) 'The surface reactivity of iron oxide nanoparticles as a potential hazard for aquatic environments: A study on Daphnia magna adults and embryos', *Scientific Reports*, 8(1), p. 13017. doi: 10.1038/s41598-018-31483-6.

Mittal, S. *et al.* (2016) 'Physico-chemical properties based differential toxicity of graphene oxide/reduced graphene oxide in human lung cells mediated through oxidative stress', *Scientific Reports*, 6(1). doi: 10.1038/srep39548.

Novoselov, K. S. *et al.* (2012) 'A roadmap for graphene', *Nature*, 490(7419), pp. 192–200. doi: 10.1038/nature11458.

Ou, L. *et al.* (2016) 'Toxicity of graphene-family nanoparticles: A general review of the origins and mechanisms', *Particle and Fibre Toxicology*. BioMed Central Ltd., pp. 1–24. doi: 10.1186/s12989-016-0168-y.

Pal, A. K. *et al.* (2014) 'Screening for oxidative damage by engineered nanomaterials: A comparative evaluation of FRAS and DCFH', *Journal of Nanoparticle Research*, 16(2). doi: 10.1007/s11051-013-2167-3.

Peijnenburg, W. J. G. M. *et al.* (2020) 'A method to assess the relevance of nanomaterial dissolution during reactivity testing', *Materials*, 13(10), p. 2235. doi: 10.3390/MA13102235.

Pelin, M. *et al.* (2018) 'Graphene and graphene oxide induce ROS production in human HaCaT skin keratinocytes: The role of xanthine oxidase and NADH dehydrogenase', *Nanoscale*, 10(25), pp. 11820–11830. doi: 10.1039/c8nr02933d.

Piątek-Guziewicz, A. *et al.* (2017) 'Ferric reducing ability of plasma and assessment of selected plasma antioxidants in adults with celiac disease', *FOLIA MEDICA CRACOVIENSIA*, 4, pp. 13–26.

Reiss, T., Hjelt, K. and Ferrari, A. C. (2019) 'Graphene is on track to deliver on its promises', *Nature Nanotechnology 2019 14:10*, 14(10), pp. 907–910. doi: 10.1038/s41565-019-0557-0.

Rogers, E. J., Bello, D. and Hsieh, S. F. (2008) 'Oxidative stress as a screening metric of potential toxicity by nanoparticles and ariborne particulate matter', *Inhalation Toxicology*. Informa Healthcare, p. 895. doi: 10.1080/08958370802020828.

Wohlleben, W. *et al.* (2019) 'The nanoGRAVUR framework to group (nano)materials for their occupational, consumer, environmental risks based on a harmonized set of material properties, applied to 34 case studies', *Nanoscale*, 11(38), pp. 17637–17654. doi: 10.1039/C9NR03306H.

Warheit, D. B., Reed, K. L. and Sayes, C. M. (2009) 'A role for nanoparticle surface reactivity in facilitating pulmonary toxicity and development of a base set of hazard assays as a component of nanoparticle risk management', *Inhalation Toxicology*, 21(SUPPL. 1), pp. 61–67. doi: 10.1080/08958370902942640.

Wiemann, M. *et al.* (2016) 'An in vitro alveolar macrophage assay for predicting the short-term

inhalation toxicity of nanomaterials', *Journal of Nanobiotechnology*, 14(1). doi: 10.1186/s12951-016-0164-2.

Zhang, H. *et al.* (2012) 'Use of Metal Oxide Nanoparticle Band Gap To Develop a Predictive Paradigm for Oxidative Stress and Acute Pulmonary Inflammation', *ACS Nano*, 6(5), pp. 4349–4368. doi: 10.1021/NN3010087.

Supplementary data 1: Physicochemical characterization

ICP Analysis

	ICP results (ppm)																						
	Al	B	Ba	Ca	Co	Cr	Cu	Fe	K	Li	Mg	Mn	Mo	Na	Ni	S	Si	Sn	Sr	Ti	V	Zn	Zr
GNP1	54	16	1	90	0	2	2	21	47	0	45	0	7	40	0	44	0	4	0	20	4	32	13
GNP2	430	92	3	538	0	1	5	1008	201	0	304	13	2	162	5	136	0	368	1	34	8	12	3
GNP3	434	97	5	147	0	26	21	589	708	0	182	6	19	420	22	421	0	32	2	108	33	8	13
GNP4	169	76	2	78	0	300	17	1015	403	0	29	32	15	162	81	2346	0	13	1	293	33	33	8
GNP5	113	58	1	40	0	275	7	1279	233	0	37	32	9	168	136	1472	0	14	0	5	9	23	5
GNP6	108	115	1	33	0	350	9	1594	196	0	37	45	9	188	175	1910	0	9	0	33	9	12	4
GNP7	87	45	1	20	0	222	5	1044	265	0	38	42	5	197	91	6464	0	9	0	138	12	13	2
GNP8	118	21	1	42	0	201	9	1068	223	0	80	29	3	135	90	12114	0	10	0	70	6	15	4
GNP9	117	61	1	122	0	231	5	1224	299	0	61	34	4	145	100	9431	0	13	0	34	7	23	3
GNP10	86	5	1	63	0	214	4	1270	173	0	36	42	4	319	100	1420	0	17	0	8	7	13	2
GNP11	184	16	1	83	0	267	8	1149	134	0	97	52	4	173	101	2085	0	6	0	5	4	22	1
GNP12	197	42	3	784	0	3	154	5980	189	0	207	29	4	73	32	3727	0	9	2	9	6	17	2
GNP13	119	72	1	65	0	0	0	524	137	28	4	5	0	76	8	20	0	7	1	16	127	22	2
GNP14	85	41	4	235	0	7	8	2373	114	0	28	19	4	47	6	28	0	9	2	23	11	30	1
GNP15	87	54	12	203	0	0	0	1173	121	0	24	6	3	46	2	44	0	9	5	35	7	16	3
rGO3	236	76	1	135	0	54	3	252	393	0	30	2058	3	98	24	156	0	307	1	3	5	221	2
rGO4	279	155	4	1315	0	7	0	151	1907	0	1257	299	66	4518	77	14679	0	14	14	3	11	599	7
rGO5	269	230	2	1661	0	64	0	215	1035	0	1369	431	15	1618	34	2819	0	196	15	68	12	55	56
rGO6	372	212	10	668	0	13	0	557	2403	0	585	1479	169	3089	658	4440	0	17	7	6	11	146	3
rGO7	235	239	3	1416	0	0	0	95	1866	0	1360	457	111	5893	53	9714	0	15	14	17	7	35	3
rGO8	463	426	3	338	0	34	9	224	1512	0	209	1907	27	862	36	5141	0	36	3	567	52	34	12
rGO9	402	165	2	256	0	23	0	215	1505	0	235	1847	23	744	38	761	0	73	2	676	51	66	7
Amorphous Silica	3223	43	19	388	0	0	0	62	90	0	49	1	2	7669	0	3356	0	5	1	24	2	7	6
CB1	136	15	1	411	0	2	0	66	221	0	152	1	0	667	1	10799	0	5	5	2	2	29	0
CB2	92	11	1	286	0	1	0	46	216	0	97	1	0	101	1	9875	0	7	1	3	0	20	0

XPS analysis

	XPS (atomic %)				
	C	O	N	S	Si
GNP1	96,8	3,2	0,0	0,0	0,0
GNP2	93,7	6,3	0,0	0,0	0,0
GNP3	92,4	7,6	0,0	0,0	0,0
GNP4	95,7	4,3	0,0	0,0	0,0
GNP5	96,7	3,3	0,0	0,0	0,0
GNP6	97,3	2,6	0,0	0,1	0,0
GNP7	95,4	4,2	0,0	0,4	0,0
GNP8	93,2	5,9	0,5	0,4	0,0
GNP9	93,2	5,7	0,7	0,3	0,0
GNP10	97,9	2,1	0,0	0,0	0,0
GNP11	97,5	2,5	0,0	0,0	0,0
GNP12	93,2	6,1	0,8	0,0	0,0
GNP13	95,6	4,4	0,0	0,0	0,0
GNP14	94,9	4,5	0,6	0,0	0,0
GNP15	96,0	3,5	0,5	0,0	0,0
rGO3	88,1	11,9	0,0	0,0	0,0
rGO4	91,7	7,2	0,0	1,0	0,0
rGO5	96,6	2,7	0,6	0,2	0,0
rGO6	84,1	15,9	0,0	0,0	0,0
rGO7	92,6	6,7	0,0	0,7	0,0
rGO8	82,8	17,2	0,0	0,0	0,0
rGO9	95,2	2,6	2,2	0,0	0,0
Amorphous Silica	96,9	2,6	0,0	0,5	0,0
CB1	97,2	2,3	0,0	0,5	0,0
CB2	3,6	70,0	0,0	0,0	26,4

RAMAN spectra

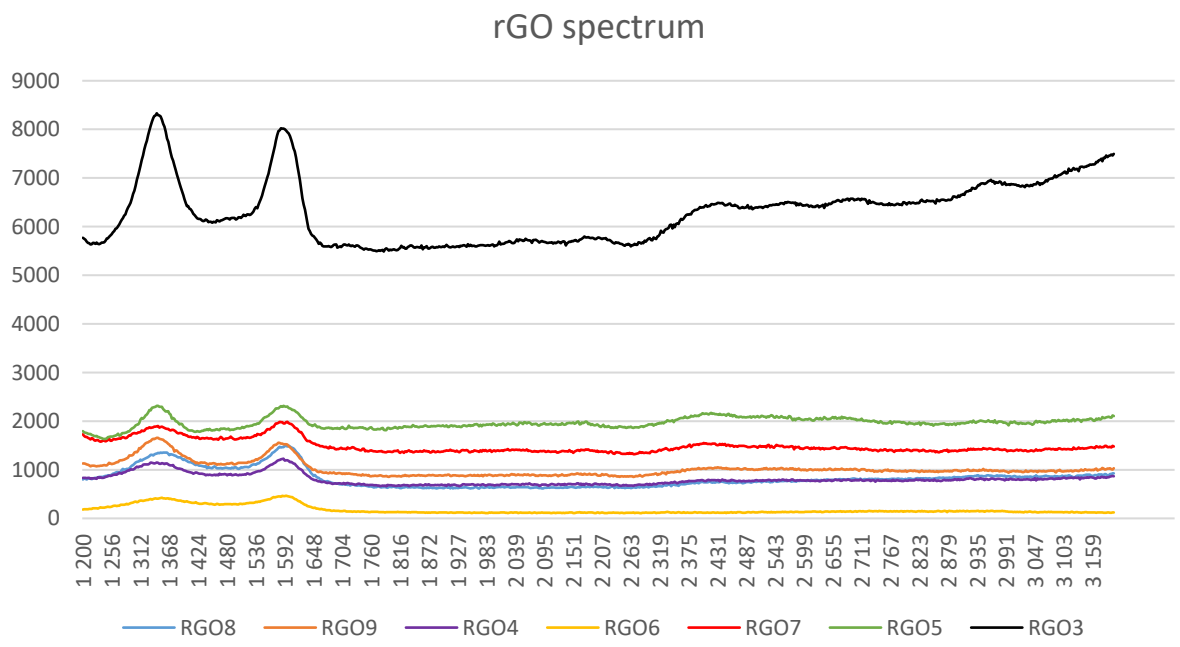

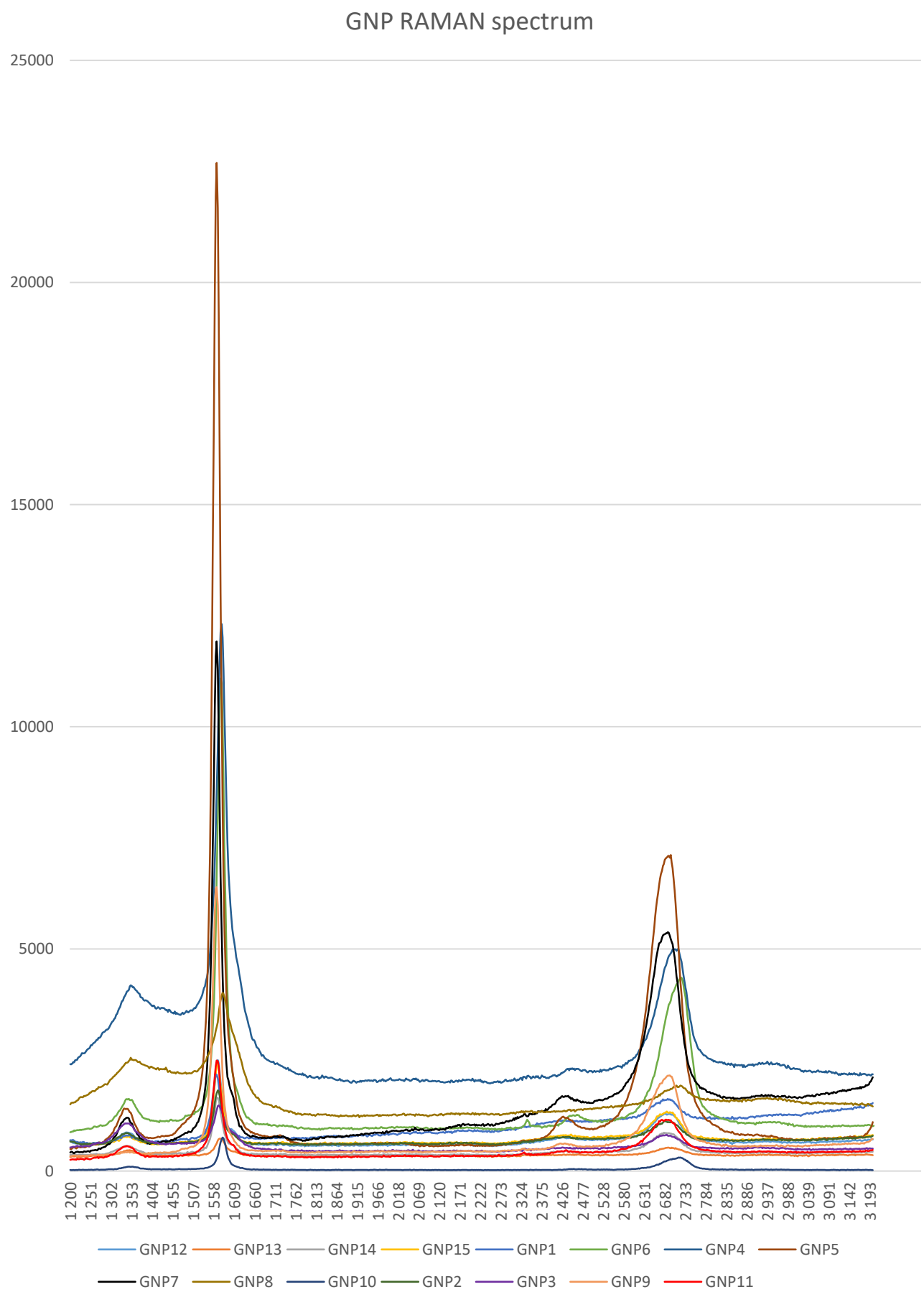
GNP RAMAN spectrum
25000
20000
15000
10000
5000
0
1 200
1 251
1 302
1 353
1 404
1 455
1 507
1 558
1 609
1 660
1 711
1 762
1 813
1 864
1 915
1 966
2 018
2 069
2 120
2 171
2 222
2 273
2 324
2 375
2 426
2 477
2 528
2 580
2 631
2 682
2 733
2 784
2 835
2 886
2 937
2 988
3 039
3 091
3 142
3 193
GNP12
GNP13
GNP14
GNP15
GNP1
GNP6
GNP4
GNP5
GNP7
GNP8
GNP10
GNP2
GNP3
GNP9
GNP11

Supplementary data 2: Presentation of the protocol and descriptive figure.

Step	Time needed	Equipment needed	Chemicals needed	Special cautions and comments	Process
Step 1 : Weight the powders	**45 minutes**	Ultraprecision Balance Centrifuge Glass tubes	Powders of nanomaterials (3 different nanomaterials can be tested in one day)	Nanopowders can be very pulverulent: use mask, protection and if possible work in a special designed lab This step can be done the day before the next steps.	Weight 7.5, 15 and 30 mg of each nanomaterials in a glass centrifuge tube. For each nanomaterial tested, one glass centrifuge tube must remain empty (blank)
Step 2 : Unfreeze the human blood serum	**15 minutes**	Heating Bath	Frozen Human Blood serum, HIV tested, aliquoted in 7mL samples	If a heating bath is not available, this step can be done at room temperature : plan approximately 40 minutes for 7 mL aliqots.	Thaw 7 mL for each nanomaterial tested (3 vials of 7 mL are thawed for a day where 3 nanomaterials are being tested).
Step 3 : Adding HBS to powders	**15 minutes**	Glass Pasteur pipette Ultraprecision Balance	Thawed Human Blood serum. Powder of nanomaterials	Nano powders can be very pulverulent : use mask, protection and if possible work in a special designed lab	Weight 1.5 g of thawed Human Blood serum to each tube containing powders, and to the empty one (blank)
To this stage, for the testing of 3 nanomaterials in one day (recommended), 12 glass centrifuges tubes should be used. Each nanomaterial groups 4 tubes: one containing only HBS (blank, C0), one containing a mix of HBS and powders at 5g/L (C5), one containing a mix of HBS and powders at 10g/L (C10), one containing a mix of HBS and powders at 20g/L (C20),					
Step 4 : Vortex and sonicate the mix HBS - powder	**15 minutes**	Sonicator Bath Vortex	Mix human blood serum - powders and Human blood serum alone (blank)	Do not forget to vortex and sonicate the blanks the same way you did with the mix Human Blood serum and powders.	For each vial : Vortex 30 seconds (3000 rpm), 20°C Sonicate in a sonicate bath 10 minutes, 130 Hz, 20°C

Step 5 : Incubation	**3 hours**	Thermo mixer (or incubator and agitator)	Mix human blood serum - powders and Human blood serum alone (blank), properly vortexed and sonicated	If a Thermomixer is no available, place an agitator in an incubator: Avoiding direct light, maintaining the samples at 37°C and a gentle agitation for 3 hours is critical.	Agitate at around 450 rpm for 3 hours, at 37°C, avoiding direct light dark, all the samples and the blanks.
Step 6 : Preparation of the FRAS reagent	**1 hour**	Ultraprecision balance	Deionized water	As the following solutions cannot be stored, they have to be prepared freshly before every experiment. Preparing S1, S2 and S3 can be done with plastic elements. However, when mixed, the final FRAS regents must be exposed to glass elements only, and have to be kept away from direct light.	**Prepare S1 :** • Weigh 0.0946 g of TPTZ in a 30 mL glass container. • Add 15 g of distilled water. • Add 1.2 mL of HCl 1M • Add distilled water to achieve a total of 30g. • Put S1 to an ultrasonication bath and sonicate for 30 minutes with maximum power at room temperature. **Prepare S2 :** • Weigh 0.2021 g of sodium acetic trihydrate in a 100 mL glass container. • Add 50 g of distilled water. • Add 1.060 mL of glacial acetic. • Add distilled water to achieve a total of 100g. **Prepare S3** : • Weigh 0.1635 g of FeCl3.6H2O in a 30 mL glass container. • Add distilled water to achieve a total of 30g. **Prepare FRAS reagent:** • Mix S1, S2 and S3 : Add 7g of S1, 7g of S3 and 70 g of S2 in a 100 mL glass container. • Store the FRAS reagent in gentle agitation (300 rpm), in the dark, room temperature, until use
			TPTZ (2,4,6-Tri(2-pyridyl)-1,3,5-triazine)		
			$FeCl_3.6H2O$		
		Agitator	glacial acetic		
			sodium acetic trihydrate		
		Sonicator Bath	1M HCl		

Step 7 : Label the reaction vials and the supernatant vials	**15 minutes**	36 10mL glass reaction vial (12 for each nanomaterial tested) 12 10 mL glass supernatant vials (4 for each nanomaterial tested)		Consider using different colors for labelling supernatant and reaction vials	Label the reaction glass vials as so : Nanomaterial code - concentration - triplicate number For instance, label AC5, AC5' and AC5'' for the reaction vials receiving the three triplicates of a 5g/L concentration of a nanomaterial A. Label the supernatant vials as so : Nanomaterial code – concentration. See supplementary figure 3 for labelling vials
Step 8 : Centrifugation*	**2 hours 30 minutes**	Centrifuge	Mix human blood serum - powders and Human blood serum alone (blank), properly vortexed and sonicated and incubated		Centrifuge at 4800 rpm for 150 minutes, at 20°C.
Step 9 : Fill every reaction vial with the FRAS reagent	**30 minutes**	2 mL glass pipette 36 10 mL reaction glass vials (12 for each nanomaterial tested)	FRAS reagent, freshly prepared (the day of the experiment)	If 2mL glass pipette is not available, you can use up to 5 mL glass pipette for maximal precision. If you don't have a graduated glass pipette, you can use Pasteur Pipette and weight 2 grams of FRAS reagent, using an ultraprecision balance. Use only glass element, and avoid direct light contact for this step.	Distribute 2mL of FRAS reagent in each of the 36 reaction glass vials.

Step 10 : Collect the supernatant *	**15 minutes**	Pasteur pipette Labelled supernatant glass vials	Mix human blood serum - powders and Human blood serum alone (blank), properly vortexed, sonicated , incubated and centrifugated.	Discard the first and the last drop to avoid any trace of nanoparticles powders in the supernatant.	Collect the supernatant of each vial. For nanoparticles of very low density, it might be necessary to add a filtration step : see section 3 of Material and Methods of the paper.
Step 11 : FRAS reaction	**1 hour**	Glass Pasteur pipette 36 mL reaction glass vials 1 mL graduated glass pipette Agitator	FRAS reagent Supernatant of the mix human blood serum - powders	If possible, use glass tips adapted to a pipetor to have a better efficiency and precision.	Every 1 minute and 30 seconds, add 100 µL of supernatant in the FRAS reagent. Let the mix FRAS reagent + supernatant incubate for 1 hour precisely, while agitating at 400 rpm, and away from direct light.
Step 12 : Absorption measurement	**1 hour**	Quartz cuvette Spectrometer Glass Pasteur Pipette	Mix FRAS regent and supernatant of HBS	An automatic linear cell changer can be useful to respect the 60 minutes timing more easily.	At precisely 60 minutes of incubation, measure the absorbance of the sample. Immediately after the measurements, rinse the quartz cuvette with distilled water, ensure you have no water left (suck in the inside of the cuvette with a Pasteur pipette) and fill it with the next sample.

Modifications compared to the protocol presented by Gandon et al.

The steps are indicated with an asterisk in the table above.

We wanted to have an insight of a potential dose-effect relationship without going through a complete screening: we then worked on 3 different exposure concentrations (5, 10 and 20 g/L instead of 0.75, 2, 5.5, 15, and 40 g/L described by Gandon *et al.*). The maximum power of our centrifuge was 4,690 rpm (instead of 11,900rpm) which was efficient enough to separate graphene-based materials powders from HBS. The use of glass components is critical for many steps as the use of plastic was found to influence the assay outcome by Gandon *et al.*, so we chose to work with glass centrifugation tubes. Lastly, we did not have an automatic cell changer in our UV/Vis spectrometer. We used the same quartz cell that we filled manually and adapted our schedule to strictly respect the required time of reaction of 60 minutes.

1. Prepare blank human blood serum (C0) and human blood serum – nanomaterial solutions (C5, C10, C20)

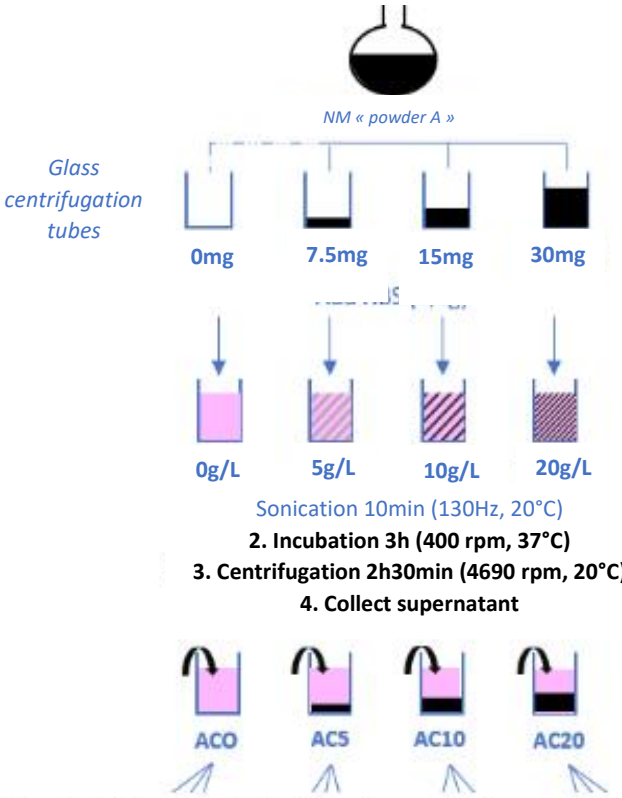

Sonication 10min (130Hz, 20°C)

2. Incubation 3h (400 rpm, 37°C)

3. Centrifugation 2h30min (4690 rpm, 20°C)

4. Collect supernatant

5. Transfer 100µL of supernatant in a glass container containing 2L of FRAS reagent

6. Incubation of 60 min

7. Read the absorbance at 500-700nm (expected peak at 593 nm)

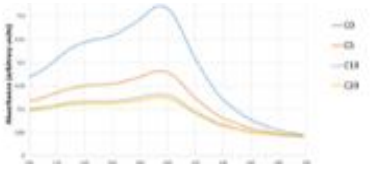

FRAS Protocol. NM: nanomaterials and HBS: human blood serum

For calibration step (done at least twice for each bottle of human blood serum you will need)

1. Prepare Trolox dilutions in water

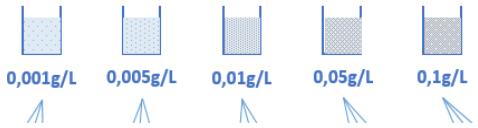

2. Transfer 100 µL of each solution in a glass container containing 2g of FRAS reagant

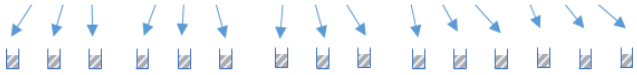

3. Incubation of 60 min

4. Read the absorbance at 500-700 nm

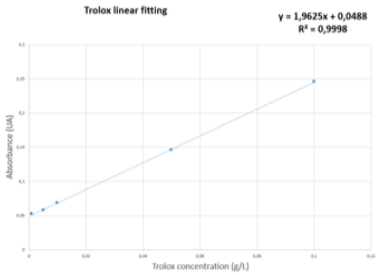

Supplementary data 3: List of equipment and chemicals used

EQUIPMENTS USED	CHEMICALS USED
ADVENTURER® PRO ANALYTICAL Balance (OHAUS)	Human serum, HIV tested (VWR)
Centrifuge glass tube, diameter 12mm and heigh 75mm with plastic cap (MC2)	Deionised water, preped with Compact Series (SG water)
Heating bath AQUALINE AL (LAUDA)	2,4,6-Tri(2-pyridyl)-1,3,5-triazine, 98% (Alfa Aesar)
Pasteur Pipette, lenght 270 mm , glass (Fisher brand)	Iron(III) chloride hexahydrate 99.0-102.0%, AnalaR Reag. Ph. Eur. analytical reagent (NORMAPUR® ACS)
ADVENTURER® PRO ANALYTICAL Balance (OHAUS)	36289 Acetic acid, glacial, ACS, 99.7+% (Afla Aesar)
Ultrasonics Bath (Branson)	Sodium acetate trihydrate 99.0-101.0%, AnalaR®, Reag. Ph. Eur. analytical reagent (NORMAPUR® ACS)
Tritramax Agitator (Heidolph)	Hydrochloric Acid Solution 1M (1N), NIST Standard Solution, ready to use, for volumetric analysis, (Fisher Chemical™)
ThermoMixer C with Thermotop (Fisher)	Manganese(III) oxide ≥98% (Alfa Aesar)
Heraeus Megafuge Centrifuge (Thermo)	6-Hydroxy-2,5,7,8-tetramethylchroman-2-carboxylic cid 97% (Acros Organics)
Spectrophotometer MULTISKAN GO + (Thermo scientific)	
Quartz cell SUPRASIL, light path 3x3mm (Hellma Analytics)	
Graduated pipettes, (2mL, Division 0,02 ml) in glass, (VWR®)	
Graduated pipettes, (1mL, Division 0,01 ml) in glass, (VWR®)	
Wizard™ Infrared Vortex Mixer (Fisherbrand™)	
Borosilicate Glass Scintillation Vials, with White Polypropylene Caps (Fisherbrand™)	
25 mm serynge filter PTFE hydrophylic, 0,2µm (Fisherbrand™)	
TERUMO SYRINGE WITHOUT NEEDLE 5mL (TERUMO)	

Supplementary data 4: Labelling the supernatant and reaction vials

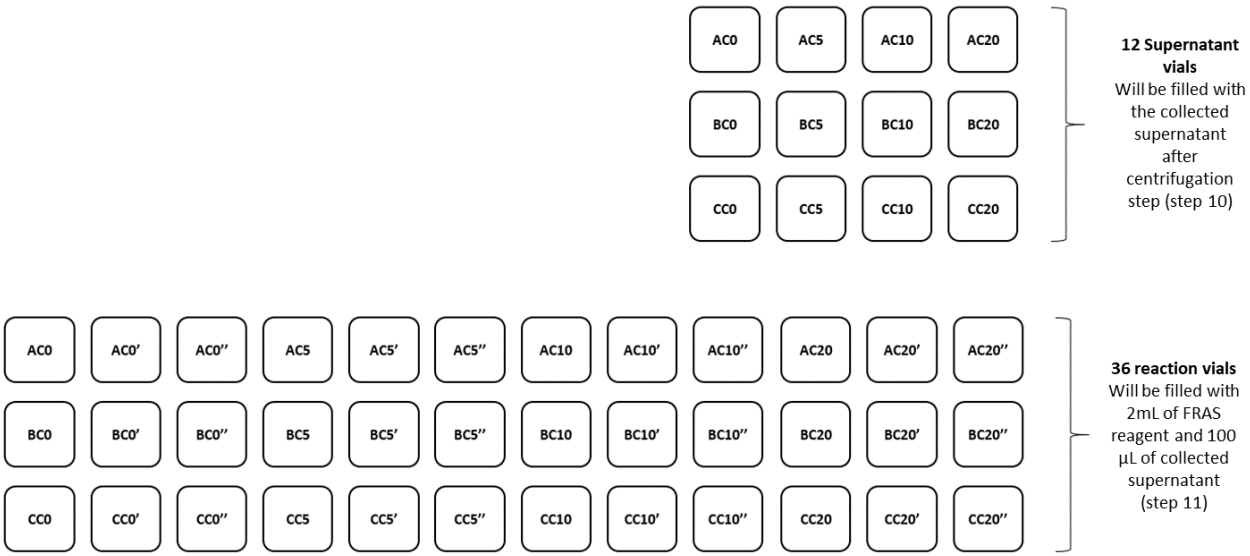

Supplementary data 5: Pictures of low-density graphene-based materials solutions and filtration.

Low density GBMs in HBS after centrifugation, 10 g/L concentration (A) and filtration (B). Please note that the filtrate should be clear.

Supplementary data 6: Explanation and example of calculations for one sample.

When we obtained the results in absorbance units, the first step was to calculate the Biological Oxidative Damage (BOD) and convert these results in Trolox Equivalent Unit (TEU). Each BOD is calculated at an exposure concentration, as presented in Equation 1. In our case, the exposure concentrations Cx were 5, 10 and 20g/L. We hence calculated a BOD_{C5}, BOD_{C10} and BOD_{C20}.

Equation 1: $BOD_{Cx} = \frac{(Abs\ at\ 593\ nm\ C-) - (Abs\ at\ 593\ nm\ Cx)}{Ke*l*d}$ [in mM TEU]

Where:

- Abs at 593 nm C- = Measured absorbance at 593 nm of the C- (blank, only HBS) solution.
- Abs at 593 nm C_x = Measured absorbance at 593 nm of the C_x solution.
- Ke*l*d = Obtained with Trolox calibration (see section 5.a).

This BOD measurement is useful for having access to the raw effect of each nanomaterials. However, for a measurement of surface reactivity, it is often necessary to introduce the specific surface area of each nanomaterial in the results, as for the surface-based BOD. We might also need to standardize the BOD with the concentration of nanomaterials used, with masse-based BOD. Then, we calculated the mass-based BOD (mBOD, see equation 2) and the surface-based BOD (sBOD, see equation 4) with the help of the Dose of nanomaterial at each concentration ($Dose_x$, see equation 3)

Equation 2: $mBOD = \frac{BOD\ cx}{cx}$ [in nM TEU /mg]

Where:

- BOD_{Cx} was calculated with equation 1 (in mMTEU)
- Cx is the exposure concentration (in g/L)

Equation 3: $Dose_x = C_x * SSA$ [in m^2/L]

Where:

- Cx is the exposure concentration (in g/L)
- SSA is the specific surface area, obtained with BET measurement (in m^2/g)

Equation 4: $sBOD = \frac{BOD\ Cx}{Dosex}$ [in nM TEU /m^2]

Where:

- BOD_{Cx} is obtained in equation 1
- $Dose_x$ is obtained in equation 3

For a better understanding of the calculations, we present a step-by-step explanation of an analysis of a specific GBM, as an example, in supplementary data 4.

		Step 1 : From Absorbance to Biological oxidative damage											
		C0			C5			C10			C20		
Absorbance measured at 593 nm	n=1	0,2948	0,3114	0,3054	0,3008	0,2991	0,2964	0,3039	0,3150	0,3218	0,2710	0,2528	0,2766
	n=2	0,3383	0,3255	0,3258	0,3122	0,3135	0,3237	0,3190	0,2795	0,3271	0,2661	0,2940	0,2811
converted in mTEU (=Abs /1.9625) *1000	n=1	150,22	158,68	155,62	153,27	152,41	151,03	154,85	160,51	163,97	138,09	128,82	140,94
	n=2	172,38	165,86	166,01	159,08	159,75	164,94	162,55	142,42	166,68	135,59	149,81	143,24

		C5			C10			C20		
BOD (Cx-C0)	n=1	-3,057	6,2675	4,586	-4,637	-1,834	-8,357	12,127	29,86	14,675
	n=2	13,299	6,1146	1,0701	9,8344	23,439	-0,662	36,79	16,051	22,777

BOD mean	C5	SD C5	C10	SD C10	C20	SD C20
	4,7134	3,8471	2,9639	9,1154	22,047	7,7622

		Step 2 : From Biological oxidative damage to mass-based Biological oxidative damage								
		C5			C10			C20		
mBOD (=BOD/C in g/L)	n=1	-0,611	1,2535	0,9172	-0,464	-0,183	-0,836	0,6064	1,493	0,7338
	n=2	2,6599	1,2229	0,214	0,9834	2,3439	-0,066	1,8395	0,8025	1,1389

mBOD mean	C5	SD C5	C10	SD C10	C20	SD C20
	0,9427	0,7694	0,2964	0,9115	1,1023	0,3881

SSA (in m^2/g)		Dose x = C (in g/L) / SSA (in m^2/g)
112	C5	22,4
	C10	11,2
	C20	5,6

		Step 2' : From Biological oxidative damage to surface-based Biological oxidative damage								
		C5			C10			C20		
sBOD (=BOD/Dosex)	n=1	-5,46	11,192	8,1893	-4,14	-1,638	-7,461	5,414	13,33	6,5514
	n=2	23,749	10,919	1,9108	8,7807	20,928	-0,591	16,424	7,1656	10,168

sBOD mean	C5	SD C5	C10	SD C10	C20	SD C20
	8,4167	6,8699	2,6463	8,1387	9,8423	3,4653

Supplementary data 7: Table presenting the previous results of the FRAS assay for graphene or carbon black materials.

	Title	Year	Authors	Studied nanomaterial	Physicochemical characteristics	BOD	sBOD	mBOD
1	Case studies putting the decision-making framework for the grouping and testing of nanomaterials (DF4nanoGrouping) into practice	2015	Josje H E Arts , Muhammad-Adeel Irfan , Athena M Keene , Reinhard Kreiling, Delina Lyon, Monika Maier , Karin Michel, Nicole Neubauer , Thomas Petry , Ursula G Sauer, David Warheit , Karin Wiench , Wendel Wohlleben , Robert Landsiedel	Graphene / Graphite nanoplatelets	N/A	With the present protocol, determination not possible due to high substance hydrophobicity		
				Low surface carbon Black	N/A	Low surface reactivity * results from Hsieh et al. (2013)		
				Various Amorphous Silica	12-20 nm (spherical)		From 5.9 to 15 nUFRAS/m²*h, classified as non-oxidative * from an unpublished report.	
2	Mapping the Biological Oxidative Damage of Engineered Nanomaterials	2013	Shu-Feng Hsieh , Dhimiter Bello , Daniel F. Schmidt , Anoop K. Pal , Aaron Stella ,Jacqueline A. Isaacs , and Eugene J. Rogers	Graphene	primary particle size = 500 nm SSA = 94-100 m²/g		92-103 sBOD [nmol TEUs/m²] Q3 classification for rank sBOD	9-10 mBOD[nmol TEUs/mg]
				Carbon Black	primary particle size=14-395 nm SSA = 8-300 m²/g		38-85 sBOD [nmol TEUs/m²] Q2 classification for rank sBOD	2-21 mBOD [nmol TEUs/mg]
				Amorphous silica	N/A		N/A	
3	Screening for oxidative damage by engineered nanomaterials: A comparative evaluation of FRAS and DCFH	2014	Anoop K. Pal, Shu-Feng Hsieh, Madhu Khatri, Jacqueline A. Isaacs, Philip Demokritou, Peter Gaines, Daniel F. Schmidt, Eugene J. Rogers & Dhimiter Bello	Graphene	N/A		N/A	
				Carbon Black	CB N110 with BET = 110,6 m²/g and primary particle size = 15nm CBN550 with BET = 39,2 m²/g and primary particle size = 44nm		CB N110 : sBOD = 85 [nmol/m²] CB N550 : sBOD = 157 [nmol/m²]	CB N110 : mBOD =9 [nmol/mg] CB N550 : mBOD = 6 [nmol/mg]
				Amorphous silica	N/A		N/A	
4	Biological oxidative damage by carbon nanotubes: Fingerprint or footprint?	2012	Shu-Feng Hsieh 1, Dhimiter Bello, Daniel F Schmidt, Anoop K Pal, Eugene J Rogers	Graphene	N/A		N/A	
				Carbon Black	N110 : 20–25 nm, BET = 110,6m²/g	BOD (mMTEU) = 0.937	sBOD (nmol /m²) = 80	mBOD (nmol /mg) = 9
				Amorphous silica	N/A		N/A	
5	Nanomaterials properties vs. biological oxidative damage: Implications for toxicity screening and exposure assessment	2009	Dhimiter Bello Shu-Feng Hsieh Daniel Frederick Schmidt Eugene Rogers	Graphene	N/A		N/A	
				Carbon Black	N110 : 15 nm, BET = 110,6m²/g N550: 44 nm, BET = 39,2m²/g N990 : >200 nm, BET = 7,7m²/g	N110 : Mean BOD [mMTEU]= 0.937 N550: Mean BOD [mMTEU]= 0.614 N990 : Mean BOD [mMTEU= 0.413		
				Amorphous silica	N/A		N/A	

Supplementary data 8: Replicability of the assay, intra and inter experiment: antioxidant capacity of the serum

Assessing our samples required a total of 360 mL of HBS which represents several bottles. Even if we ordered the same reference with the same supplier, we wanted to be sure that we did not have a significant variability of its total antioxidant capacity depending on the batch, for example. For each nanomaterial testing, we measured the absorbance of the HBS alone. We found that its antioxidant capacity was stable, with a value of 168.6 ± 6.64 µMTEU.

However, we observed a slight variation with the values obtained in previous papers (Gandon *et al*., Hiesh *et al.*,) where these values were respectively 366µMTEU and 530 µMTEU (for the last value, it was indicated 530 mMTEU but we assume it was a typo).

While remaining very stable through our experiments, it appears that the grade and source of the serum has a notable influence on its total antioxidant capacity. The biological oxidative damage is based on the relative change between the non-exposed HBS and the exposed HBS, lowering the impact of this variability. However, we recommend working on the same reference of HBS when possible and to assess the antioxidant capacity of the HBS regularly during the testing.